Supporting Information for the manuscript titled "Deposition of *Cryptosporidium parvum* Oocysts in Porous Media: A Synthesis of Attachment Efficiencies Measured under Varying Environmental Conditions"

Yeonjeong Park [a], Thomas Harter [b] *, E. Robert Atwill [c], Lingling Hou [d], Aaron I. Packman [e]

[a b] Land, Air, and Water Resources, University of California, One Shields Ave, Davis, 95616-8628, USA

[c] School of Veterinary Medicine, , University of California, One Shields Ave, Davis, 95616-8734, USA

[d] Kearney Agricultural Center, 9240 S. Riverbend Avenue, Parlier, California 93648, USA

[e] Civil and Environmental Engineering, Northwestern University, 2145 Sheridan Road, Evanston, IL 60208-3109, USA

* Corresponding author email: tharter@ucdavis.edu tel: 530-752-2709, fax: 530-752-5262

The number of pages: 12 (excluding cover sheet)

The number of figures: 3

The number of tables: 3

Colloid Filtration Theory

Colloid Filtration Theory has been employed to design water treatment plant filtration processes [1, 2] and in modeling colloid transport in natural granular porous media [3, 4]. A body of physical/chemical theory for the interactions of particles, collectors, and fluid flow supports CFT [5-8]. The deposition of colloidal particles is often represented as a first-order, steady-state process [6]:

$$\frac{dC}{dx} = -\lambda C \tag{1}$$

where C is particle concentration, x is the longitudinal coordinate (flow direction), and λ is the filtration coefficient [1/L]. Equation (1) can be expressed using α and η as follows [8]:

$$\frac{dC}{dx} = -\frac{3}{2}\frac{(1-\varepsilon)^{1/3}}{d_c}\alpha\eta C \tag{2}$$

where ε is the porosity of the bed and d_c is the collector (grain) diameter. The exponent 1/3 is used since η term is multiplied by $(1-\varepsilon)^{2/3}$ [9]. Then the filtration coefficient can be defined as:

$$\lambda = \frac{3}{2}\frac{(1-\varepsilon)^{1/3}}{d_c}\alpha\eta \tag{3}$$

Integrating equation (2) yields:

$$\ln\frac{C}{C_0} = -\frac{3}{2}\frac{(1-\varepsilon)^{1/3}}{d_c}\alpha\eta L \tag{4}$$

where C_0 and L are the initial particle concentration and the bed depth, respectively. In this study, η is estimated using equations in Table S1. *C. parvum* breakthrough curve data are then used to calculate α from (3). The filtration coefficient, λ, can be employed in the advection-dispersion equation to describe the temporal and spatial distribution of particle concentration within the porous medium as follows:

$$\frac{\partial C}{\partial t} = D\frac{\partial^2 C}{\partial x^2} - v\frac{\partial C}{\partial x} - \lambda v C \tag{5}$$

where D is the dispersion coefficient, and v is the interstitial fluid velocity.

Collector Efficiency (η)

The approach mechanisms of colloid particles from the bulk of the fluid to the porous medium (collector) surface are divided into three separate processes, diffusion, interception, and sedimentation [8]:

$$\eta = \eta_D + \eta_I + \eta_G \quad (6)$$

where η_D, η_I, are η_G represent single collector efficiencies by diffusion, interception, and gravity respectively. These three mechanisms have been modeled by Rajagopalan and Tien[10], Tufenkji and Elimelech [11], and Nelson and Ginn [12], referred to as RT, TE, and NG models in this paper.

Rajagopalan and Tien [10] enhanced the accuracy of the collector efficiency model initially developed by Yao et al. [8] by incorporating effects of London van der Waals forces and hydrodynamic retardation on interception and sedimentation processes. The RT model also modified the impact of neighboring grains and the effect of porosity in a packed bed, which was not accounted for in the model by Yao et al. [8]. The original analysis was performed for an isolated spherical single collector. Tufenkji and Elimelech [11] developed a new collector efficiency model by also evaluating effects of London van der Waals forces and hydrodynamic retardation on the diffusion process, not only on the interception and sedimentation process. They incorporated the mechanisms related to colloid particle approach to collectors in a multiple linear regression analysis where constants of power functions of multiple dimensionless parameters were estimated (e.g., $\eta_I = aN_R^b N_{Pe}^c N_{vdW}^d$, where *a*-*d* are constants). Regression input data were developed using a fully Eulerian solution of the ADE (equation 5) and a wide range of parameter values relevant to most applications in aquatic systems [11]. Nelson and Ginn [12] later found that the RT and TE equations may underestimate colloid approach in saturated porous media due to the use of improper boundary conditions (RT and TE models), i.e., imposing power law dependence of collector efficiency on the Peclet and gravity numbers, and due to the differences in the numerical treatment of the hydrodynamic retardation effect. The NG model introduced correction factors for the diffusion and sedimentation terms to provide an appropriate asymptotic approach to unity for the collector efficiency, otherwise η values calculated from the RT and TE models become larger than one as the Peclet number decreases and the gravity number increases. They employed a fully Lagrangian scheme to solve the ADE and then applied nonlinear regression analysis to estimate the correlation between η and the multiple dimensionless numbers.

Table S1. The RT, TE, and NG models for estimating single collector efficiency, η, expressed in terms of dimensionless parameters for collisions by diffusion, interception, and gravitational mechanisms.

	η_D	η_I	η_G
RT	$4\,A_s^{1/3} N_{pe}^{-2/3}$	$A_s N_{Lo}^{1/8} N_R^{15/8}$	$0.00338\,A_s N_G^{1.2} N_R^{-0.4}$
TE	$2.4 A_s^{1/3} N_R^{-0.081} N_{pe}^{-0.715} N_{vdw}^{0.052}$	$0.55 A_s N_R^{1.55} N_{pe}^{-0.125} N_{vdw}^{0.125}$	$0.22 N_R^{-0.24} N_G^{1.11} N_{vdw}^{0.053}$
NG	$2.4\,A_s^{1/3}\left[\frac{N_{pe}}{N_{pe}+16}\right]^{0.75} N_{pe}^{-0.68} N_{Lo}^{0.015} N_{Gi}^{0.8}$	$A_s N_{Lo}^{1/8} N_R^{15/8}$	$0.7\left[\frac{N_{Gi}}{N_{Gi}+0.9}\right] N_G N_R^{-0.05}$

where η_D, η_I, and η_G represent single collector efficiencies by diffusion, interception, and gravity, respectively, $N_R = \frac{d_p}{d_c}$, $N_{pe} = \frac{U\,d_c}{D_p}$, $N_{Lo} = \frac{4H}{9\pi\mu d_p^2 U}$, $N_{vdw} = \frac{H}{kT}$, $N_G = \frac{U_p}{U}$, and $N_{Gi} = \frac{1}{N_G + 1}$ are dimensionless numbers for interception, Peclet, London force, Van der Waals, gravitation, and modified gravitation respectively. A_s is $\frac{2(1-\gamma^5)}{2-3\gamma+3\gamma^5-2\gamma^6}$, γ is $(1-\varepsilon)^{1/3}$, d_p is particle diameter, U is the fluid approach velocity, D_p is particle diffusion coefficient, $D_p = \frac{kT}{3\pi\mu d_p}$, H is the Hamaker constant, μ is the fluid viscosity, k is the Boltzman constant, U_p is the settling velocity, $U_p = \frac{g(\rho_p - \rho_f) d_p^2}{18\mu}$, g is the gravitational acceleration, ρ_p is the particle density, and ρ_f is the fluid density. Each η_D, η_I, and η_G term is multiplied by γ^2 to calculate total collector efficiencies.

Collision (Attachment) Efficiency (α)

Once a particle approaches a collector and if there is no repulsive interaction between the particle and collector, deposition (attachment) occurs [13]. The kinetics of colloid attachment are controlled by solution chemistry and the chemical characteristics such as surface charge of particles or collectors[13]. Changes in solution chemistry - modifying concentration of salts or pH of the solution - determine surface charge characteristics of particles. These changes in electrical potential are correlated with colloid stability and can be measured by the zeta potential of the colloid surface [13].

The interaction of colloid particles with collectors that lead to attachment can be classified into DLVO and non-DLVO interactions [13]. DLVO theory quantifies colloidal surface-surface interaction caused by van der Waals attraction and electrical double layer repulsion [13]. It has been extensively used to explain colloid stability [13, 14]. In an electrolyte solution, the distribution of ions around a charged particle is balanced by an equivalent number of oppositely charged counterions. The surface charge on a particle and the associated counterion

charge together constitute the electrical double layer, which greatly depends on the solution chemistry and surface potentials of the colloids and collectors [13]. The attractive force that always exists between colloidal particles is generally called the London-van der Waals force which arises from spontaneous electrical and magnetic polarizations. The Hamaker approach [15] is based on the assumption of pairwise additivity of intermolecular forces. It has been used to evaluate the London-van der Waals force in practical applications.

Colloidal interaction involves non-DLVO forces such as hydrophobic effects that provide additional attraction between particles and collectors, or steric repulsion that arises from the presence of adsorbed polymers on the particle surface [13]. These additional processes affect attachment in ways that may result in large discrepancies between DLVO theory-based values of attachment efficiency and experimental data [16, 17]. The presence of an adsorbed layer can alter the electrical double layer force or interparticle van der Waals attraction [13]. The non-DLVO influence on the colloid stability has yet to be mathematically and systematically established [13]. Further, the chemical heterogeneities of colloid and mineral grain surfaces give rise to unfavorable chemical conditions in natural sediments, which makes the prediction of colloid deposition pattern more intractable [14]. Therefore, α is typically determined empirically with calculated η and observed C_{max}/C_0 from experimental breakthrough curve data.

Calculation of α using DLVO theory

The DLVO interactions involve two forces, electrical double layer (EDL) repulsion and van der Waals (VDW) attraction. The total energy of interaction can be calculated by summing of these two energies. Most particles in water are charged and carry an electrical double layer. As two charged particles approach each other in water, the diffuse parts of their double layers begin to overlap and this causes an interaction. The interaction between charged particles depends on the zeta potential which is commonly used to calculate EDL interaction between two spheres as follows [18]:

$$V_E = 2\pi\varepsilon\zeta_1\zeta_2 \frac{d_1 d_2}{d_1 + d_2} \exp(-\kappa h)$$

where ε is the permittivity of water, ζ_1 and ζ_2 are zeta potentials of a collector and a colloid particle at pH 7 respectively, d_1 and d_2 are diameters of a collector and a colloid particle, κ is Debye-Huckel length, and h is separation distance. For zeta potentials of the same sign, V_E is positive, so the interaction is always repulsive, which is the case in our experiment. When the salt concentration or ionic strength in water varies, both the zeta potential and the Debye-Huckel length (κ) are affected. It is customary to refer to $1/\kappa$ as the "thickness" of the diffuse

double layer (range of repulsion) [19]. Addition of inert electrolyte increases κ and decreases the thickness of the diffuse double layer.

Between all atoms and molecules there are attractive forces referred to as van der Waals force. Van der Waals force includes dipole-dipole forces which occur in molecules that have an unequal sharing of electrons and dispersion forces which exist between nonpolar molecules, but induced dipoles [18]. The van der Waals energy of attraction between two spheres per unit area can be estimated as follows [18]:

$$V_A = -\frac{A_{12}}{12h}\frac{d_1 d_2}{(d_1 + d_2)}$$

where A_{12} is Hamaker constant which depends on the properties of different materials, 1 and 2. Calculated van der Waals, electrical, and total interaction energy at 3mM NaCl and pH 7 is shown in Figure S1.

It appeared that non-DLVO forces existed in our experiment with the water at high ionic strength (100mM NaCl). However, our analysis with existing experimental data from the literature demonstrated that α has strong linear relationship with ionic strength and pH as long as DLVO theory holds (where non-DLVO forces do not exist). Ionic strength and pH are directly related to zeta potential change, which will affect the total interaction energy. Therefore, α can be estimated by easily obtainable solution chemistry, ionic strength and pH if no other chemical treatment on colloids and collectors is involved. Ionic strength is represented by Debye-Huckel length (κ) in this study as follows [20]:

$$\kappa = \left(\frac{2N_A e_0^2 I}{\varepsilon_0 \varepsilon_r kT} \right)^{\frac{1}{2}}$$

where N_A is Avogadro's number, e_0 is elementary charge, I is ionic strength, ε_0 is permittivity of free space, ε_r is dielectric constant of water, k is Boltzmann constant, and T is absolute temperature.

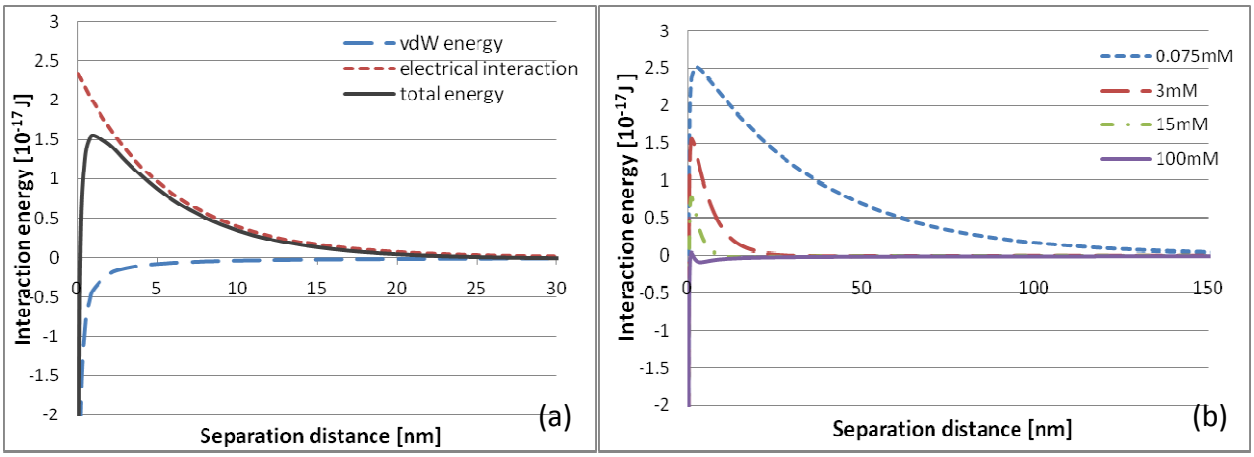

Figure S1. (a) Calculated DLVO interaction energy between *C. parvum* oocyst and Accusand with respect to separation distance at ionic strength of 3mM NaCl and pH 7. (b) Estimated DLVO interaction energy at different ionic strengths. Secondary minimum exists where separation distance is larger than 280nm, 29nm, 10nm, and 2nm at ionic strength of 0.075mM, 3mM, 15mM, and 100mM respectively. Hamaker constant of 10^{-20} J was used. Zeta potential of Accusand was obtained from Attinti et al. [21] and zeta potential of *C. parvum* oocyst was measured.

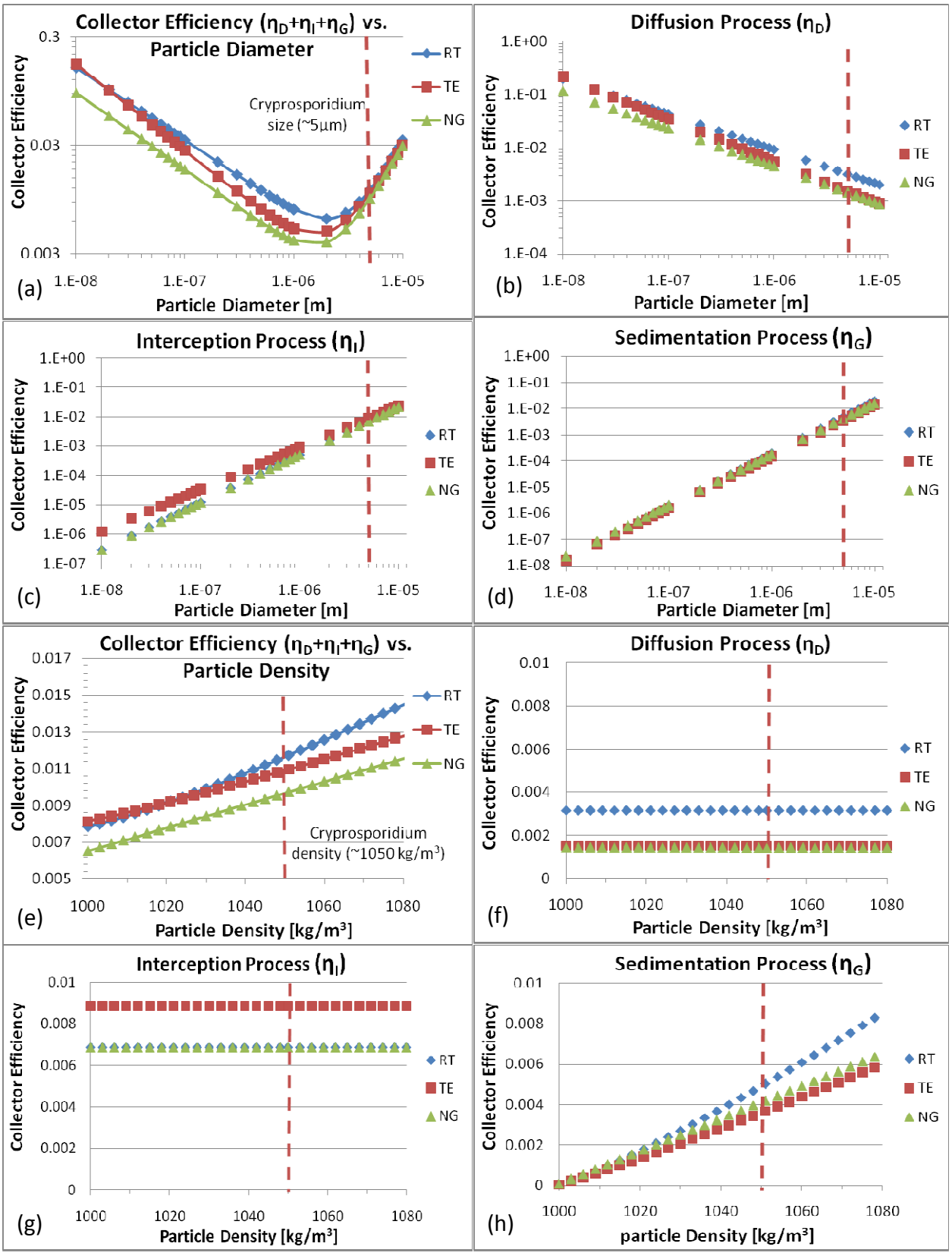
Collector Efficiency ($\eta_D+\eta_I+\eta_G$) vs. Particle Diameter
Collector Efficiency
Particle Diameter [m]
Cryprosporidium size (~5µm)
RT
TE
NG
(a)
Diffusion Process (η_D)
(b)
Interception Process (η_I)
(c)
Sedimentation Process (η_G)
(d)
Collector Efficiency ($\eta_D+\eta_I+\eta_G$) vs. Particle Density
Particle Density [kg/m³]
Cryprosporidium density (~1050 kg/m³)
(e)
Diffusion Process (η_D)
(f)
Interception Process (η_I)
(g)
Sedimentation Process (η_G)
particle Density [kg/m³]
(h)

Figure S2. (a) Calculated collector efficiency involved with diffusion, interception, and sedimentation processes ($\eta_D + \eta_I + \eta_G$), (b) diffusion process (η_D), (c) interception process (η_I), and (d) sedimentation process (η_G) with respect to particle diameter. (e) $\eta = \eta_D + \eta_I + \eta_G$, (f) η_D, (g) η_I, and (h) η_G with respect to particle density. Approach velocity is 8.22×10^{-5}, collector diameter is 4.25×10^{-4}, and porosity is 0.31. Other parameter values in Table S3 are used. Dashed vertical line indicates the size of *C. parvum* oocyst in (a)~(d) and the density of *C. parvum* oocyst in (e) ~ (h).

Table S2. Hypothesis testing (two-sided t test) results of the significance in difference between α_{RT} and α_{NG} (largest numerical difference). Note: Two-tail t test with two independent samples (α_{RT} and α_{NG}) was conducted. Null hypothesis is that α_{RT} and α_{NG} have equal means. This test assumes that the variances of α_{RT} and α_{NG} are the same. The threshold chosen for statistical significance was 0.05 level.

exp #	Feature	t value	p value	df	Mean difference	Standard deviation	CV*	Confidence interval	Reject?
1	3mM	- 0.99	0.33	20	-0.059	0.14	-2.37	-0.18, 0.065	no
2	0.075mM	-0.54	0.59	24	-0.017	0.079	-4.72	-0.08, 0.047	no
3	15mM	-6.24	1.32×10^{-6}	26	-0.17	0.074	-0.42	-0.23, -0.12	yes
4	100mM	-0.48	0.64	22	-0.018	0.094	-5.09	-0.098, 0.061	no
5	9mM ($MgCl_2$)	-0.65	0.52	18	-0.027	0.093	-3.42	-0.11, 0.06	no
6	pH 5.5	-3.34	0.0018	40	-0.1	0.1	-0.97	-0.17, -0.041	yes
7	pH 8.5	-0.89	0.39	18	-0.045	0.12	-2.52	-0.15, 0.062	no
8	Iron coating	-1.11	0.28	22	-0.079	0.17	-2.2	-0.23, 0.068	no
9	illite	-2.55	0.02	18	-0.072	0.063	-0.88	-0.13, -0.013	yes

*Coefficient of Variation

Verification of multiple regression model, α

In an effort to verify the regression model, experimental data from Harter et al. [22], Hsu et al. [23], Tufenkji et al. [24], Tufenkji and Elimelich [25], Bradford and Bettahar [26], Kim et al. [27], and our experiments were used for multiple regression analysis and the three data from Dai and Hozalski [28], Abudalo et al. [29], and Abudalo et al. [30] were selected to check if the regression model can be implemented with these three experimental data. The resulted equations for the multiple regression are presented in Figure S3. Verification results (in Figure S3) demonstrate that the multiple regression model can predict α sufficiently well with other experimental data.

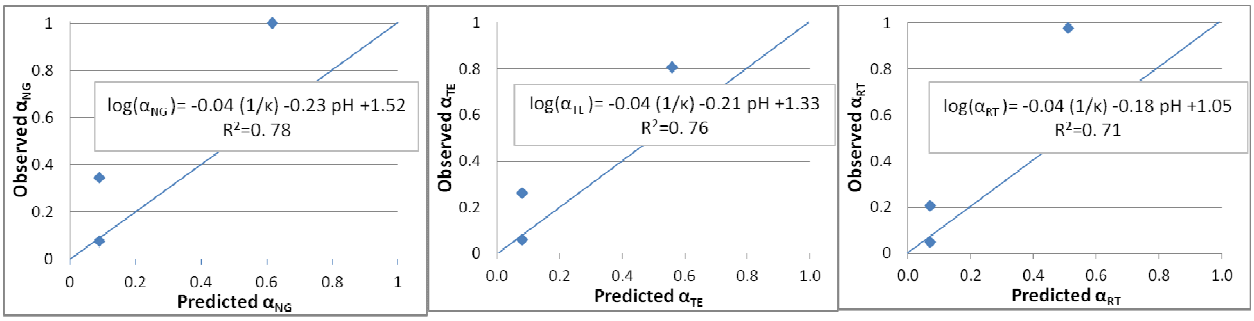

Figure S3. Verification of multiple regression equation with three experimental data.

Table S3. Parameter values employed to calculate collector efficiencies and attachment efficiencies. If not specified in papers, educated guesses or calculated values based on other information are assigned.

Citation		Particle diameter [m]	Column length [m]	Hamaker constant [kg m^2/s^2]	Viscosity of water [kg m/s]	Temperature [˚K]	Particle density [kg/m^3]	Water density [kg/m^3]
Brush et al. 1999 [31]		5×10^{-6}	0.109	1×10^{-20}	1×10^{-3}	293	1070	999
Harter et al. 2000 [22]		5×10^{-6}	0.1	1×10^{-20}	9.4×10^{-4}	296	1080	999
Hsu et al. 2001 [23]	glassbeads	5×10^{-6}	0.1	1.2×10^{-21}	8.94×10^{-4}	298	1080	998
	polystyrene			1.15×10^{-21}				
Logan et al. 2001 [4]		5×10^{-6}	0.6	1×10^{-20}	1.25×10^{-3}	288	1050	999
Dai and Hozalski 2002 [28]		5×10^{-6}	0.25	1×10^{-20}	8.94×10^{-4}	296	1080	998
Tufenkji et al. 2004 [24]		3.6×10^{-6}	0.071	6.5×10^{-21}	1.01×10^{-3}	295	1047	1000
Tufenkji and Elimelech 2005 [25]		4.3×10^{-6}	0.126	6.5×10^{-21}	1.01×10^{-3}	293	1047	1000
Abudalo et al. 2005 [29]		3.6×10^{-6}	0.1	6.5×10^{-21}	1×10^{-3}	293	1075	998
Bradford and Bettahar 2005 [26]	Sand 710 µm	4×10^{-6}	0.13	6.5×10^{-21}	1.01×10^{-3}	293	1050	1000
	Sand 360 µm		0.126					
	Sand 150 µm		0.127					
Hijnen et al. 2005 [32, 33]		4.9×10^{-6}	0.5	6.2×10^{-21}	1.11×10^{-3}	286	1045	999.703
Hijnen et al. 2007 [34]		4.9×10^{-6}	1.5	6.2×10^{-21}	1.25×10^{-3}	295	1045	999.703
Abudalo et al. 2010 [30]		3.6×10^{-6}	0.1	6.5×10^{-21}	9.8×10^{-4}	293	1075	998
This study		5×10^{-6}	0.2	1×10^{-20}	9.4×10^{-4}	296	1050	999

Literature Cited

1. Ramaley, B. L.; Lawler, D. F.; Wright, W. C.; Omelia, C. R., Integral Analysis of Water-Plant Performance. *J. Environ. Eng.-Asce* **1981,** *107*, (3), 547-562.
2. Omelia, C. R., Particles, Pretreatment, and Performance in Water Filtration. *J. Environ. Eng.-Asce* **1985,** *111*, (6), 874-890.
3. Harvey, R. W.; Garabedian, S. P., Use of Colloid Filtration Theory in Modeling Movement of Bacteria through a Contaminated Sandy Aquifer. *Environ. Sci. Technol.* **1991,** *25*, (1), 178-185.
4. Logan, A. J.; Stevik, T. K.; Siegrist, R. L.; Ronn, R. M., Transport and fate of Cryptosporidium parvum oocysts in intermittent sand filters. *Water Res.* **2001,** *35*, (18), 4359-4369.
5. von Smoluchowski, M., Versuch einer mathematischen Theorie der koagulationskinetik Kolloider Lösungen. *Z. Phys. Chem* **1918,** *92*, 129-168.
6. Iwasaki, T., Some notes on sand filtration. *J. Am. Water Work Assoc.* **1937,** *29*, 1591-1602.
7. Happel, J., Viscous Flow in Multiparticle Systems - Slow Motion of Fluids Relative to Beds of Spherical Particles. *Aiche J.* **1958,** *4*, (2), 197-201.
8. Yao, K. M.; Habibian, M. M.; Omelia, C. R., Water and Waste Water Filtration - Concepts and Applications. *Environ. Sci. Technol.* **1971,** *5*, (11), 1105-&.
9. Logan, B. E.; Jewett, D. G.; Arnold, R. G.; Bouwer, E. J.; Omelia, C. R., Clarification of Clean-Bed Filtration Models. *J. Environ. Eng.-ASCE* **1995,** *121*, (12), 869-873.
10. Rajagopalan, R.; Tien, C., Trajectory Analysis of Deep-Bed Filtration with Sphere-in-Cell Porous-Media Model. *Aiche J.* **1976,** *22*, (3), 523-533.
11. Tufenkji, N.; Elimelech, M., Correlation equation for predicting single-collector efficiency in physicochemical filtration in saturated porous media. *Environ. Sci. Technol.* **2004,** *38*, (2), 529-536.
12. Nelson, K. E.; Ginn, T. R., New collector efficiency equation for colloid filtration in both natural and engineered flow conditions. *Water Resour. Res.* **2011,** *47*, (W05543), doi:10.1029/2010WR009587.
13. Elimelech, M.; Gregory, J.; Jia, X.; Williams, R. A., *Particle Deposition and Aggregation: measurement, modeling and simulation*. Butterworth-Heinemann: Oxford, England, 1995.
14. Ryan, J. N.; Elimelech, M., Colloid mobilization and transport in groundwater. *Colloid Surface A* **1996,** *107*, 1-56.
15. Hamaker, H. C., The London - Van Der Waals attraction between spherical particles. *Physica* **1937,** *4*, 1058-1072.
16. Elimelech, M.; Omelia, C. R., Effect of Particle-Size on Collision Efficiency in the Deposition of Brownian Particles with Electrostatic Energy Barriers. *Langmuir* **1990,** *6*, (6), 1153-1163.
17. Elimelech, M.; Omelia, C. R., Kinetics of Deposition of Colloidal Particles in Porous-Media. *Environ. Sci. Technol.* **1990,** *24*, (10), 1528-1536.
18. Gregory, J., *Particles in water; Properties and Processes*. IWA Pub.Taylor & Francis: Boca Raton, FL, 2005; p 180.
19. Shaw, D. J., *Electrophoresis*. Academic P.: London, New York,, 1969; p viii, 144.
20. Debye, P.; Huckel, E., The theory of electrolytes I. The lowering of the freezing point and related occurrences. *Physikalische Zeitschrift* **1923,** *24*, 185-206.
21. Attinti, R.; Wei, J.; Kniel, K.; Sims, J. T.; Jin, Y., Virus' (MS2, phi X174, and Aichi) Attachment on Sand Measured by Atomic Force Microscopy and Their Transport through Sand Columns. *Environ Sci Technol* **2010,** *44*, (7), 2426-2432.
22. Harter, T.; Wagner, S.; Atwill, E. R., Colloid transport and filtration of Cryptosporidium parvum in sandy soils and aquifer sediments. *Environ. Sci. Technol.* **2000,** *34*, (1), 62-70.
23. Hsu, B. M.; Huang, C. P.; Pan, J. R., Filtration behaviors of Giardia and Cryptosporidium - Ionic strength and pH effects. *Water Res.* **2001,** *35*, (16), 3777-3782.

24. Tufenkji, N.; Miller, G. F.; Ryan, J. N.; Harvey, R. W.; Elimelech, M., Transport of Cryptosporidium oocysts in porous media: Role of straining and physicochemical filtration. *Environ. Sci. Technol.* **2004,** *38*, (22), 5932-5938.
25. Tufenkji, N.; Elimelech, M., Spatial distributions of Cryptosporidium oocysts in porous media: Evidence for dual mode deposition. *Environ. Sci. Technol.* **2005,** *39*, (10), 3620-3629.
26. Bradford, S. A.; Bettahar, M., Straining, attachment, and detachment of Cryptosporidium oocysts in saturated porous media. *J. Environ. Qual.* **2005,** *34*, (2), 469-478.
27. Kim, H. N.; Walker, S. L.; Bradford, S. A., Coupled factors influencing the transport and retention of Cryptosporidium parvum oocysts in saturated porous media. *Water Res* **2010,** *44*, (4), 1213-1223.
28. Dai, X. J.; Hozalski, R. M., Effect of NOM and biofilm on the removal of Cryptosporidium parvum oocysts in rapid filters. *Water Res.* **2002,** *36*, (14), 3523-3532.
29. Abudalo, R. A.; Bogatsu, Y. G.; Ryan, J. N.; Harvey, R. W.; Metge, D. W.; Elimelech, M., Effect of ferric oxyhydroxide grain coatings on the transport of bacteriophage PRD1 and Cryptosporidium parvum oocysts in saturated porous media. *Environ. Sci. Technol.* **2005,** *39*, (17), 6412-6419.
30. Abudalo, R. A.; Ryan, J. N.; Harvey, R. W.; Metge, D. W.; Landkamer, L., Influence of organic matter on the transport of Cryptosporidium parvum oocysts in a ferric oxyhydroxide-coated quartz sand saturated porous medium. *Water Res* **2010,** *44*, (4), 1104-1113.
31. Brush, C. F.; Ghiorse, W. C.; Anguish, L. J.; Parlange, J. Y.; Grimes, H. G., Transport of Cryptosporidium parvum oocysts through saturated columns. *J. Environ. Qual.* **1999,** *28*, (3), 809-815.
32. Hijnen, W. A. M.; Brouwer-Hanzens, A. J.; Charles, K. J.; Medema, G. J., Transport of MS2 phage, Escherichia coli, Clostridium perfringens, Cryptosporidium parvum and Giardia intestinalis in a gravel and a sandy soil. *Environ. Sci. Technol.* **2005,** *39*, (20), 7860-7868.
33. Hijnen, W. A. M.; Brouwer-Hanzens, A. J.; Charles, K. J.; Medema, G., Transport of MS2 phage, Escherichia coli, Clostridium perfringens, Cryptosporidium parvum, and Giardia intestinalis in a gravel and a sandy soil. (vol 39, pg 7860, 2005). *Environ. Sci. Technol.* **2006,** *40*, (4), 1371-1371.
34. Hijnen, W. A. M.; Dullemont, Y. J.; Schijven, J. F.; Hanzens-Brower, A. J.; Rosielle, M.; Medema, G., Removal and fate of Cryptosporidium paruum, Clostridium perfringens and small-sized centric diatoms (Stephanodiscus hantzschii) in slow sand filters. *Water Res.* **2007,** *41*, (10), 2151-2162.